

ELECTRON TRANSPORT THROUGH QUANTUM DOTS: AN UNUSUAL KONDO EFFECT

S. De Franceschi^a, S. Sasaki^b, J. M. Elzerman^a, W. G. van der Wiel^a,
M. Eto^{a,c}, S. Tarucha^{b,d}, and L. P. Kouwenhoven^a

^a *Department of Applied Physics, DIMES, and ERATO Mesoscopic Correlation Project,
Delft University of Technology, PO Box 5046, 2600 GA Delft, The Netherlands*

^b *NTT Basic Research Laboratories,
Atsugi-shi, Kanagawa 243-0198, Japan*

^c *Faculty of Science and Technology, Keio University,
3-14-1 Hiyoshi, Kohoku-ku, Yokohama 223-8522, Japan*

^d *ERATO Mesoscopic Correlation Project, University of Tokyo,
Bunkyo-ku, Tokyo 113-0033, Japan*

Quantum-dot devices consist of a small electronic island connected by tunnel barriers to source and drain electrodes [1]. Due to on-site Coulomb repulsion, the addition of an electron to the island implies an energy change $U=e^2/C$, where C is the total capacitance of the island. Hence the number of confined electrons is a well-defined integer, N , that can be controlled by varying the voltage on a nearby gate electrode. Transport of electrons through the dot is allowed only at the transition points where the N - and $(N+1)$ -states are both energetically accessible. Otherwise, N is constant and current transport is strongly suppressed. As a result, the linear conductance as a function of gate voltage exhibits a sequence of narrow resonances located at the transitions between consecutive electron numbers. This is known as Coulomb blockade [2,3]. If the tunnel conductance of the barriers, G_t , is much smaller than the quantum conductance, e^2/h , transport can be well described in terms of single-electron processes, which are first-order in G_t . As G_t approaches $\sim e^2/h$, however, higher-order tunneling events need to be taken into account. These are commonly known as *co-tunneling* events since they involve the simultaneous coherent tunneling of two or more

electrons [4]. In the case of spin-less electrons, the co-tunneling contribution to conductance can be evaluated by perturbation theory. The leading term is a second-order in G . A more complicated scenario occurs when the spin degree of freedom is taken into account. If the total spin of the quantum dot is non-zero, the coherent superposition of virtual tunnel events can result in a strong correlation between the localised electrons and the free electrons in the leads. The physics of a quantum dot becomes similar to the physics of a magnetic impurity in a metal host, i.e. the Kondo effect.

In metal alloys, the Kondo effect manifests itself as an increased resistivity at low temperatures. This anomalous behaviour was discovered over sixty years ago and remained for a long time an open question. In 1964 J. Kondo established the relation between the temperature dependence of the resistivity and the exchange interaction between a localised spin and conduction electrons [5]. The Kondo effect is now recognised as a key mechanism in a wide class of correlated electron systems [6,7]. Control over single, localised spins has become relevant also in fabricated structures due to the rapid developments in nano-electronics [8,9]. Two years ago the Kondo effect was observed in artificial, quantum-dot structures. In these systems, the Kondo effect yields an enhancement of the conductance, G , which may reach the unitary limit ($G=2e^2/h$) at low temperatures. The dots studied previously by Goldhaber-Gordon *et al.* [10], by ourselves [11], and other groups [12,13], all contained several tens of electrons, their number being not precisely known. These observations fitted reasonably well within the existing understanding.

In the present manuscript we investigate Kondo physics in a few-electron quantum dot in which we know the quantum numbers of the occupied electron states. Besides the normal Kondo effect for spin equal to 1/2 and odd electron number, we also observe an unexpected Kondo effect for an even electron number. This novel effect occurs at the degeneracy between singlet and triplet states. The characteristic energy scale is found to be much larger than for the ordinary spin-1/2 case.

The total spin of a quantum dot is zero or an integer for $N = \text{even}$ and half-integer for $N = \text{odd}$. The latter case constitutes the canonical example for the Kondo effect [14,15] when all electrons can be ignored, except for the one with the highest energy; i.e. the case of a single, isolated spin, $S = 1/2$ (see Fig. 1(a)). Although the energy level ε_0 is well below the Fermi energies of the two leads, Heisenberg uncertainty allows the electron on the dot to tunnel to one of the leads when it is replaced quickly by another electron. The time scale for such a co-tunneling process is $\sim \hbar/U$. Figure 1(a) illustrates that particle exchange by co-tunneling can effectively flip the spin on the dot. At low temperature, the coherent superposition of all possible co-tunneling

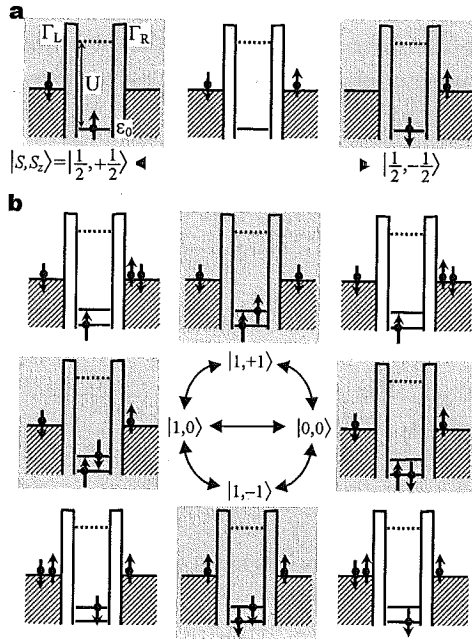


Figure 1. Spin-flip processes leading to ordinary and singlet-triplet Kondo effect in a quantum dot. (a) Co-tunneling event in a spin-1/2 quantum dot for $N = \text{odd}$. Only the highest-energy electron is shown occupying a single spin-degenerate level, ϵ_0 . (The case of two, or more, closely spaced levels has also been considered theoretically within the context of the spin-1/2 Kondo effect¹⁶.) The gray panels refer to $S_z = 1/2$ and $-1/2$ ground states, which are coupled by a co-tunneling event. The two tunnel barriers have tunneling rates Γ_R and Γ_L . In the Coulomb blockade regime ($|\epsilon_0| \sim U$) adding or subtracting an electron from the dot implies an energy cost $\sim U$. Hence the intermediate step (diagram in the middle) is a high-energy, virtual state. The spin-flip event depicted here is representative of a large number of higher-order processes which add up coherently such that the local spin is screened. This Kondo effect leads to an enhanced linear-response conductance at temperatures below T_K . (b) Co-tunneling in an integer-spin quantum dot for $N = \text{even}$ at a singlet-triplet degeneracy. Two electrons can share the same orbital with opposite spins (singlet state in the gray panel on the right) or occupy two distinct orbitals in one of the three spin-triplet configurations (top, left, and bottom gray panels). The different spin states are coupled by virtual states (intermediate diagrams). Similar to the spin-1/2 case, spin-flip events can screen the local magnetic moment. Note that an $S = 1$ Kondo effect only involves $|1, +1\rangle$, $|1, 0\rangle$, and $|1, -1\rangle$.

processes involving spin flip can result in a time-averaged spin equal to zero. The whole system, i.e. quantum dot plus electrodes, forms a spin singlet. The energy scale for this singlet state is the Kondo temperature, T_K . In terms of

density of states, a narrow peak with a width $\sim k_B T_K$ develops at the Fermi energy. Note that for $N = \text{even}$ and $S = 0$, co-tunneling gives rise to a lifetime broadening of the confined state, without producing any Kondo resonance. Such even/odd behaviour corresponding to no-Kondo/Kondo has been observed in recent experiments [10,11].

It is also possible that a quantum dot with $N = \text{even}$ has a total spin $S = 1$; e.g. when the last two electrons have parallel spins. If the remaining $N-2$ electrons can be ignored, this corresponds to a triplet state. Parallel spin filling is a consequence of Hund's rule occurring when the gain in exchange energy exceeds the spacing between single-particle states [17]. The spin of the triplet state can also be screened by co-tunneling events. These are illustrated in the center-left side of Fig. 1(b). In contrast to single-particle states that are considered in the spin-1/2 Kondo problem, the spin triplet consists of three degenerate two-particle states. Co-tunneling exchanges only one of the two electrons with an electron from the leads. The total spin of the many-body Kondo state depends on how many modes in the leads couple effectively to the dot [18,19]. If there is only one mode, the screening is not complete and the whole system does not reach a singlet state. In this case the Kondo effect is called "underscreened". Calculations show that also for $S = 1$ a narrow Kondo resonance arises at the Fermi energy, however, the corresponding T_K is typically lower than in the case of $S = 1/2$ [20,21]. Some experiments have reported the absence of even/odd behaviour [22,23], which may be related to the formation of higher spin states.

Here, we investigate a quantum dot with $N = \text{even}$ where the last two electrons occupy a degenerate state of a spin singlet and a spin triplet. Figure 1(b) illustrates the different co-tunneling processes occurring in this special circumstance. Starting from $|S = 1, S_z = 1\rangle$, where S_z is the z -component of the total spin on the dot, co-tunneling via a virtual state $|1/2, 1/2\rangle$, can lead either to the triplet state $|1, 0\rangle$, or to the singlet state $|0, 0\rangle$. Via a second co-tunneling event the state $|1, -1\rangle$ can be reached. As for the $S = 1$ case, the local spin can fluctuate by co-tunneling events. By coupling to all triplet states, the singlet state enhances the spin exchange interaction between the dot and the leads, resulting in a higher rate for spin fluctuations. This particular situation yields a strong Kondo effect, which is characterised by an enhanced T_K . This type of Kondo effect has not been considered before, probably because a singlet-triplet degeneracy does not occur in magnetic elements. Recent scaling calculations indeed indicate a strong enhancement of T_K at the singlet-triplet degeneracy [25]. Ref. [24] also argues that the total spin of the many-body Kondo state behaves as in the case of $S = 1$.

Our quantum dot has the external shape of a rectangular pillar (see Fig. 2(a,b)) and an internal confinement potential close to a two-dimensional ellipse [25]. The tunnel barriers between the quantum dot and the source and

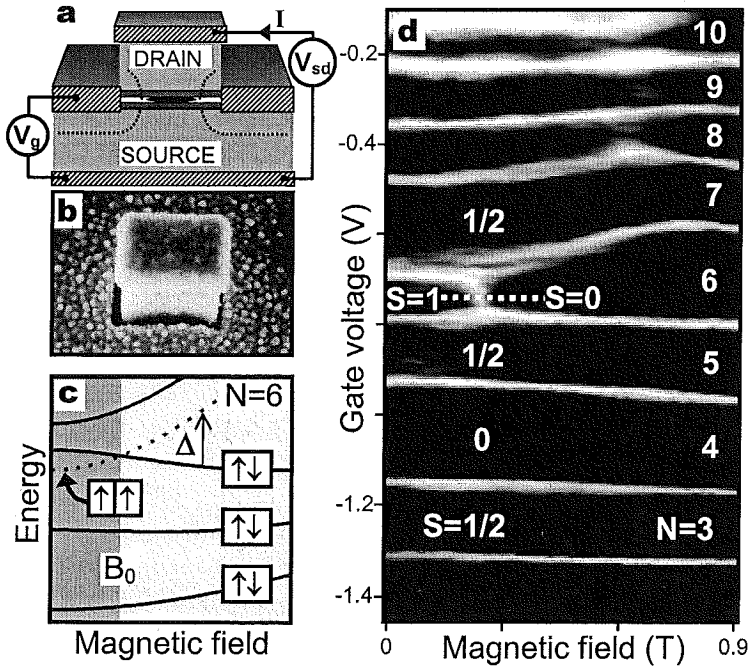


Figure 2. (a) Cross-section of our rectangular quantum dot. The semiconductor material consists of an undoped AlGaAs(7nm)/InGaAs(12nm)/AlGaAs(7nm) double barrier structure sandwiched between n-doped GaAs source and drain electrodes. A gate electrode surrounds the pillar and is used to control the electrostatic confinement in the quantum dot. A dc bias voltage, V_{sd} , is applied between source and drain and current, I , flows vertically through the pillar. In addition to V_{sd} , we apply a modulation with rms amplitude $V_{ac} = 3 \mu\text{V}$ at 17.7 Hz for lock-in detection. The gate voltage, V_g , can change the number of confined electrons, N , one-by-one from ~ 10 at $V_g = 0$ to 0 at $V_g = -1.8$ V. A magnetic field, B , is applied along the vertical axis. Temperature, T , is varied between 14 mK and 1 K. The lowest effective electron temperature is 25 ± 5 mK. (b) Scanning electron micrograph of a quantum dot with dimensions $0.45 \times 0.6 \mu\text{m}^2$ and height of $\sim 0.5 \mu\text{m}$. (c) Schematic energy spectrum. Solid lines represent the B -evolution of the first four orbital levels in a single-particle model. The dashed line is obtained by subtracting the two-electron exchange coupling from the fourth level. At the crossing between this dashed line and the third orbital level at $B = B_0$ the ground state for $N = 6$ undergoes a triplet-to-singlet transition. $B_0 \approx 0.22$ T with a slight dependence on V_g . We define Δ as the energy difference between the triplet and the singlet states. (d) Gray-scale representation of the linear conductance versus V_g and B . White stripes denote conductance peaks of height $\sim e^2/h$. Dark regions of low conductance indicate Coulomb blockade. The $N = 6$ ground state undergoes a triplet-to-singlet transition at $B_0 \approx 0.22$ T, which results in a conductance anomaly inside the corresponding Coulomb gap.

drain electrodes are thinner than in our previous devices [17,25] such that co-tunneling processes are enhanced. Figure 2(d) shows the linear response conductance (dc bias voltage $V_{sd} = 0$) versus gate voltage, V_g , and magnetic field, B . Dark regions have low conductance and correspond to the regimes of Coulomb blockade for $N = 3$ to 10. In contrast to previous experiments [10,11,12,13] on the Kondo effect, all performed on lateral quantum dots with unknown electron number, here the number of confined electrons is precisely known. The stripes represent Coulomb peaks as high as $\sim e^2/h$. The B -dependence of the first two lower stripes reflects the ground-state evolution for $N = 3$ and 4. Their similar B -evolution indicates that the 3rd and 4th electron occupy the same orbital state with opposite spin, which is observed also for $N = 1$ and 2 (not shown). This is not the case for $N = 5$ and 6. The $N = 5$ state has $S = 1/2$, and the corresponding stripe shows a smooth evolution with B . Instead, the stripe for $N = 6$ has a kink at $B \approx 0.22$ T. From earlier analysis [25] and from measurements of the excitation spectrum at finite V_{sd} (discussed below) we can identify this kink with a transition in the ground state from a spin triplet to a spin singlet. Strikingly, at the triplet-singlet transition (at $B = B_0$ in Fig. 2(c)) we observe a strong enhancement of the conductance. In fact, over a narrow range around 0.22 T, the Coulomb gap for $N = 6$ has disappeared completely.

To explore this conductance anomaly, we show in Fig. 3(a) differential conductance measurements, dI/dV_{sd} versus V_{sd} , taken at $B = B_0$ and V_g corresponding to the dotted line in Fig. 2(d). At $T = 14$ mK the narrow resonance around zero bias has a full-width-at-half-maximum, FWHM ≈ 30 μ V. This is several times smaller than the lifetime broadening, $\Gamma = \Gamma_R + \Gamma_L \approx 150$ μ V, as estimated from the FWHM of the Coulomb peaks. The height of the zero-bias resonance decreases logarithmically with T (see Fig. 3(b)). These are typical fingerprints of the Kondo effect. From FWHM $\approx k_B T_K$, we estimate $T_K \approx 350$ mK. We note that we can safely neglect the Zeeman spin splitting since $g\mu_B B_0 \approx 5$ μ V $\ll k_B T_K$, implying that the spin triplet is in fact three-fold degenerate at $B = B_0$. This condition is essential to the Kondo effect illustrated in Fig. 1(b). Alternative schemes have recently been proposed for a Kondo effect where the degeneracy of the triplet state is lifted by a large magnetic field [26,27]. Some of the traces in Fig. 3(a) also show some small short-period modulations which disappear above ~ 200 mK. These are due to a weak charging effect in the GaAs pillar above the dot [28].

For $N = 6$ we find markedly anomalous T -dependence only when singlet and triplet states are degenerate. Away from degeneracy, the valley conductance increases with T due to thermally activated transport. For $N = 5$ and 7, zero-bias resonances are clearly observed (see insets to Fig. 3(a))

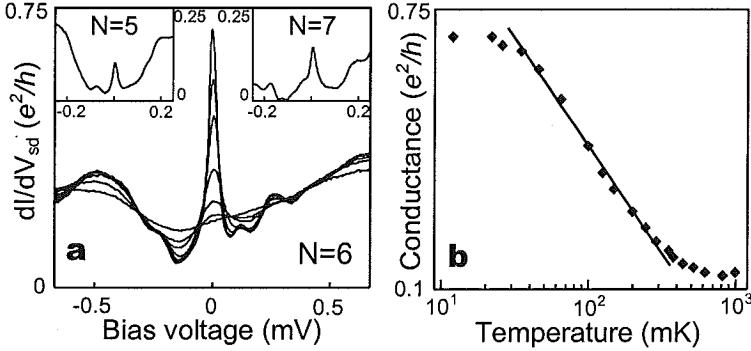


Figure 3. (a) Kondo resonance at the singlet-triplet transition. The dI/dV_{sd} versus V_{sd} curves are taken at $V_g = -0.72$ V, $B = 0.21$ T and for $T = 14, 65, 100, 200, 350, 520,$ and 810 mK. Insets to (a): Kondo resonances for $N = 5$ (left inset) and $N = 7$ (right inset), measured at $V_g = -0.835$ V and $V_g = -0.625$ V, respectively, and for $B = 0.11$ T and $T = 14$ mK. (b) Peak height of zero-bias Kondo resonance versus T as obtained from (a) (solid diamonds). The line demonstrates a logarithmic T -dependence, which is characteristic for the Kondo effect. The saturation at low T is likely due to electronic noise.

which are related to the ordinary spin-1/2 Kondo effect. Their height, however, is much smaller than for the singlet-triplet Kondo effect.

We now investigate the effect of lifting the singlet-triplet degeneracy by changing B at a fixed V_g corresponding to the dotted line in Fig. 2(d). Near the edges of this line, i.e. away from B_0 , the Coulomb gap is well developed as denoted by the dark colours. The dI/dV_{sd} versus V_{sd} traces still exhibit anomalies, however, now at finite V_{sd} (see Fig. 4(a)). For $B = 0.21$ T we observe the singlet-triplet Kondo resonance at $V_{sd} = 0$. At higher B this resonance splits apart showing two peaks at finite V_{sd} . It is important to note that these peaks occur inside the Coulomb gap. They result from “inelastic” co-tunneling events, where “inelastic” refers to exchanging energy between the dot and the electrodes [4] (see also the lower panel in Fig. 4(b)). The upper traces in Fig. 4(a), for $B < 0.21$ T, also show peak structures, although less pronounced.

Inelastic co-tunneling occurs when $eV_{sd} = \pm\Delta$, and this condition is independent of V_g . We believe that for small Δ the split resonance reflects the singlet-triplet Kondo anomaly shifted to finite bias. This resembles the splitting of the Kondo resonance by the Zeeman effect [10,11,29], although on a very different B -scale. In the present case, the splitting occurs between two different multi-particle states and originates from the B -dependence of the orbital motion. For increasing Δ , the shift to larger V_{sd} induces spin-

decoherence processes, which broaden and suppress the finite-bias peaks [29]. For $B \approx 0.39$ T the peaks have evolved into steps [30] which may indicate that the spin-coherence associated with the Kondo effect has completely vanished.

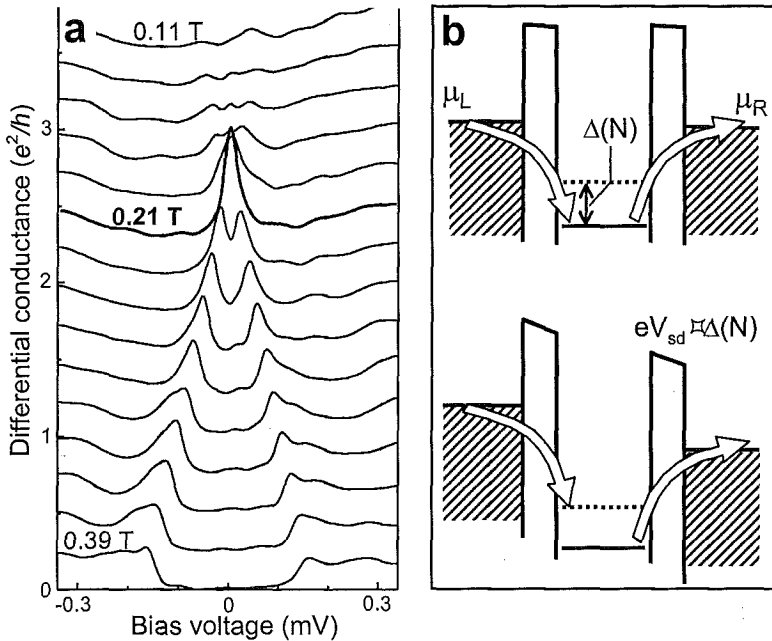


Figure 4. (a) dI/dV_{sd} versus V_{sd} characteristics taken along the dotted line in Fig. 2d ($V_g = -0.72$ V) at equally spaced magnetic fields $B = 0.11, 0.13, \dots, 0.39$ T. Curves are offset by $0.25 e^2/h$. (b) Schematic energy diagrams illustrating two different types of co-tunneling processes: “elastic” co-tunneling (top), which leaves the dot in its ground state (solid level), and “inelastic” co-tunneling (bottom), which brings it into an excited state (dotted level). The latter process is allowed only for an applied bias, eV_{sd} , exceeding the lowest excitation energy for N electrons on the dot, $\Delta(N)$. Although it is called “inelastic”, the total electron energy is conserved, while the on-site excitation is created at the expense of the energy drop eV_{sd} .

Acknowledgements

We thank Yu. V. Nazarov, K. Majjala, S. M. Cronenwett, J. E. Mooij, and Y. Tokura for discussions. We acknowledge financial support from the Specially Promoted Research, Grant-in-Aid for Scientific Research, from the Ministry of Education, Science and Culture in Japan, from the Dutch Organisation for Fundamental Research on Matter (FOM), from the NEDO joint research program (NTDP-98), and from the EU via a TMR network.

References

- [1] L.P. Kouwenhoven *et al.*, in *Mesoscopic Electron Transport*, edited by L.L. Sohn, L.P. Kouwenhoven, and G. Schön, (Kluwer, Series E 345, 1997), p.105.
- [2] D.V. Averin and K.K. Likharev, in *Mesoscopic Phenomena in Solids*, edited by B.L. Altshuler *et al.*, (Elsevier, Amsterdam, 1991), p. 173.
- [3] C.W.J. Beenakker, *Phys. Rev. B* **44**, 1646 (1991).
- [4] D.V. Averin and Yu. V. Nazarov, in *Single Charge Tunneling - Coulomb Blockade Phenomena in Nanostructures*, edited by H. Grabert and M.H. Devoret (Plenum Press, New York, 1992), p. 217.
- [5] J. Kondo, *Prog. Theor. Phys.* **32**, 37 (1964).
- [6] A.C. Hewson, *The Kondo Problem to Heavy Fermions* (Cambridge University Press, Cambridge, 1993).
- [7] D.L. Cox and M.B. Maple, *Physics Today* **48**, 32 (1995).
- [8] G.A. Prinz, *Science* **282**, 1660-1663 (1998).
- [9] D. Loss and D.P. DiVincenzo, *Phys. Rev. A* **57**, 120 (1998).
- [10] D. Goldhaber-Gordon *et al.*, *Nature* **391**, 156 (1998).
- [11] S.M. Cronenwett, T.H. Oosterkamp, and L.P. Kouwenhoven, *Science* **281**, 540 (1998).
- [12] J. Schmid *et al.*, *Physica B* **256-258**, 182 (1998).
- [13] F. Simmel *et al.*, *Phys. Rev. Lett.* **83**, 804 (1999).
- [14] L.I. Glazman, and M.E. Raikh, *JETP Lett.* **47**, 452 (1988).
- [15] T.K. Ng, and P.A. Lee, *Phys. Rev. Lett.* **61**, 1768 (1988).
- [16] T. Inoshita *et al.*, *Phys. Rev. B* **48**, 14725 (1993).
- [17] S. Tarucha *et al.*, *Phys. Rev. Lett.* **84**, 2485 (2000).
- [18] D.C. Mattis, *Phys. Rev. Lett.* **19**, 1478 (1967).
- [19] P. Nozières and A. Blandin, *J. Physique* **41**, 193 (1980).
- [20] Y. Wan, P. Phillips, and Q. Li, *Phys. Rev. B* **51**, 14782 (1995).
- [21] W. Izumida, O. Sakai, and Y. Shimizu, *J. Phys. Soc. Jpn.* **67**, 2444 (1998).
- [22] S.M. Maurer *et al.*, *Phys. Rev. Lett.* **83**, 1403 (1999).
- [23] J. Schmid *et al.*, *Phys. Rev. Lett.* **84**, 5824 (2000).
- [24] M. Eto and Yu. V. Nazarov, *Phys. Rev. Lett.* **85**, 1306 (2000).
- [25] D.G. Austing *et al.*, *Phys. Rev. B* **60**, 11514 (1999).
- [26] M. Pustilnik, Y. Avishai, and K. Kikoin, *Phys. Rev. Lett.* **84**, 1756 (2000).
- [27] D. Giuliano and A. Tagliacozzo, *Phys. Rev. Lett.* **84**, 4677 (2000).
- [28] The top contact is obtained by deposition of Au/Ge and annealing at 400 °C for 30 s. This thermal treatment is gentle enough to prevent the formation of defects near the dot, but does not allow the complete suppression of the native Schottky barrier. The residual barrier leads to electronic confinement and corresponding charging effects in the GaAs pillar.
- [29] N.S. Wingreen and Y. Meir, *Phys. Rev. B* **49**, 11040 (1994).
- [30] Y. Funabashi *et al.*, *Jpn. J. Appl. Phys.* **38**, 388 (1999).

